Biomedicine & Pharmacotherapy 184 (2025) 117871

Contents lists available at ScienceDirect

Biomedicine & Pharmacotherapy

journal homepage: www.elsevier.com/locate/biopha

Activation of α7nAch receptors ameliorates α-synuclein pathology in the brain and gut of a subacute MPTP mouse model of Parkinson's disease

Yea-Hyun Leem [a,1], Jung-Eun Park [a,1], Jin-Sun Park [a], Do-Yeon Kim [a], Jae-Min Park [a], Seong-Eun Kim [a], Jihee Lee Kang [b], Hee-Sun Kim [a,*]

[a] Department of Molecular Medicine and Inflammation-Cancer Microenvironment Research Center, School of Medicine, Ewha Womans University, Seoul, South Korea
[b] Department of Physiology and Inflammation-Cancer Microenvironment Research Center, School of Medicine, Ewha Womans University, Seoul, South Korea

ARTICLE INFO

Keywords:
Parkinson's disease
α7nAchR
α-synuclein pathology
Gut-brain axis
Anti-inflammation

ABSTRACT

Parkinson's disease (PD) is a neurological disorder that causes a gradual decrease in mobility. Abnormal α-synuclein (α-syn) levels and aggregation contribute to PD development. The dissemination of α-synuclein pathology via the gut-brain axis has emerged as a critical aspect in α-synucleinopathies, including PD. Recently, α7 nicotinic acetylcholine receptor (α7nAchR) agonists have been proposed as promising agents for treating PD, owing to their biological properties such as anti-inflammatory effects. This study aims to investigate whether activation of α7nAchR improves α-synuclein pathology in the brain and gut of a mouse model of PD. We found that α7nAchR agonists, GTS-21 and PNU-282987, induced behavioral recovery and improved nigrostriatal dopaminergic neurotransmission in a subacute MPTP mouse model of PD. In addition, GTS-21 and PNU-282987 facilitated α-syn clearance in the brain and distal colon, as evidenced by a considerable reduction in the accumulation of pathogenic forms of α-syn. Accordingly, GTS-21 and PNU-282987 were found to promote the AMPK-mTOR autophagy signaling pathway. Furthermore, GTS-21 and PNU-282987 exerted anti-inflammatory effects, reducing the levels of proinflammatory mediators such as inducible nitric oxide synthase, interleukin-6, and tumor necrosis factor-α in both the brain and gut. To validate the specific effects of α7nAchR agonists, subacute MPTP mice were pretreated with methyllycaconitine (MLA), a selective α7nAchR antagonist before GTS-21 administration. Pretreatment with MLA abolished the GTS-21-elicited behavioral recovery, α-syn clearance, and anti-inflammatory effects in the brain and gut. Therefore, α7nAchR activation may be a potential candidate strategy for the treatment of PD by altering α-syn aggregation in the brain and gut.

1. Introduction

Parkinson's disease (PD) is a prevalent neurological disorder that manifests both motor and nonmotor symptoms. Deficient nigrostriatal dopaminergic neurotransmission, persistent neuroinflammation, and formation of Lewy bodies (LB) composed primarily of misfolded α-synuclein (α-syn) aggregates are the hallmarks of PD [1]. α-syn is a small cytoplasmic protein found mostly at presynaptic terminals. It regulates synaptic vesicle release, recycling, and neural plasticity [2,3]. Mutations, multiplication, and polymorphisms of the *SNCA* gene contribute to the pathophysiology of α-synucleinopathies, such as PD [4,5]. According to numerous studies, pathophysiological α-syn species, including insoluble aggregates and oligomeric species, disrupt axonal transport; cause mitochondrial dysfunction, oxidative stress, synaptic dysfunction, and endoplasmic reticulum/Golgi dysfunction; and activate microglia, eventually leading to neuroinflammation [6–8]. To

Abbreviations: AMPK, AMP-activated protein kinase; α7nAchR, α7 nicotinic acetylcholine receptor; α-syn, alpha-synuclein; DMV, dorsal motor nucleus of vagus nerve; ENS, enteric nervous system; GFAP, glial fibrillary acidic protein; Iba-1, ionized calcium-binding adapter molecule 1; IL-6, interleukin-6; INOS, inducible nitric oxide synthase; LB, Lewy body; MLA, methyllycaconitine; MPTP, 1-methyl-4-phenyl-1,2,3,6-tetrahydropyridine; MPTP/P, MPTP/probenecid; mTOR, mammalian target of rapamycin; NF-κB, nuclear factor-κB; Nrf2, nuclear factor erythroid 2-related factor 2; PD, Parkinson's disease; PNU, PNU-282987; SN, substantia nigra; SNpc, substantia nigra pars compacta; TH, tyrosine hydroxylase; Thio-S, thioflavin-S; TNF-α, tumor necrosis factor-alpha.

* Correspondence to: Department of Molecular Medicine, School of Medicine, Ewha Womans University, 808-1 Magok-dong, Gangseo-gu, Seoul 07804, South Korea.
E-mail address: hskimp@ewha.ac.kr (H.-S. Kim).
[1] These authors contributed equally to this work

https://doi.org/10.1016/j.biopha.2025.117871
Received 8 October 2024; Received in revised form 22 January 2025; Accepted 23 January 2025
Available online 1 February 2025
0753-3322/© 2025 The Author(s). Published by Elsevier Masson SAS. This is an open access article under the CC BY license (http://creativecommons.org/licenses/by/4.0/).

counteract the etiology of PD, pharmacological strategies targeting α-syn abnormalities are being currently explored.

Multiple evidence have indicated the prion-like transmission of α-syn in experimental models and clinical studies [9–12]. For example, endocytosis-mediated cell-to-cell transfer of oligomeric or fibrillar α-syn resulted in worsening damages to recipient cells, leading to apoptosis [11,13]. In this context, LB have been detected in diverse brain structures, including substantia nigra (SN), dorsal motor nucleus of vagus nerve (DMV), and locus coeruleus, as well as the enteric nervous system (ENS) and submandibular glands [14]. In patients with PD presenting with gastrointestinal symptoms, neuropathology evaluation revealed the presence of misfolded α-syn-containing inclusions in the ENS, including colonic submucosal and DMV neurons [15,16]. These observations corroborated the hypothesis by Braak that α-syn propagates from the ENS to the brain through the vagus nerve and DMV within the medulla oblongata [17,18]. Therefore, targeting α-syn pathology across the gut-to-brain axis is a promising approach for preventing and treating PD.

Cholinergic deficits are implicated in a myriad of PD symptoms [19]. Most intestinal cholinergic axons in the distal gut express α-syn selectively, with the pathogenic process of PD also involving degenerative alterations and the loss of cholinergic neurons [20]. Furthermore, the central cholinergic neurons and cholinergic innervated vagus nerve system are the primary pathways through which pathogenic α-syn propagates in the gut-brain axis [21]. A recent study found that α7 nicotinic acetylcholine receptor (α7nAchR) agonists, such as nicotine and PNU-282987 (PNU), reduced mitochondrial-dependent apoptosis and pathogenic α-syn accumulation in α-syn preformed fibril-treated SH-SY5Y cells [22]. In addition, long-term MPTP injection increased α-syn deposits and caused dopaminergic neuron death in α7nAchR knockout mice. These findings suggested that activating α7nAchR may help improve α-syn pathology. Furthermore, the cholinergic anti-inflammatory pathway connects the innate immune system to the parasympathetic nerve system [23]. α7nAchR is present in immune cells such macrophages, astrocytes, microglia, and monocytes. Activating this system is known to suppress the generation of proinflammatory cytokines, commonly known as the nicotinic anti-inflammatory pathway [24–26].

GTS-21 (3-[2,4-dimethoxybenzylidene]-anabaseine, DMXBA), a synthetic benzylidene derivative of the naturally found anabaseine, is one of the most potent α7nAchR agonist [27]. GTS-21, a blood-brain barrier-permeable compound, promotes microglial Aβ phagocytosis and anti-inflammatory activity [28,29]. PNU is a strong and selective agonist of neuronal α7nAchR that exerts nootropic effects [30]. In terms of PD pathology, PNU reduces dopaminergic cell loss and neuroinflammation in the context of MPTP- and 6-hydroxydopamine-induced neurotoxicity [31,32]. However, little empirical evidence exist to suggest that α7nAchR agonists improve bidirectional gut-brain connection in α-synucleinopathy. To investigate the role of α7nAchR activation in PD-related pathophysiology, PD model mice were administered two powerful agonists (GTS-21 and PNU), following the MPTP paradigm. We evaluated whether activating α7nAchR accelerated α-syn clearance and decreased inflammation in the colon and brain of a subacute MPTP animal model of PD.

2. Materials and methods

2.1. Reagents and antibodies

GTS-21 was obtained from Abcam (Cambridge, UK). PNU-282987 and MLA were purchased from Sigma-Aldrich (St. Louis, MO, USA). 1-methyl-4-phenyl-1,2,3,6-tetrahydropyridine (MPTP) was purchased from Tokyo Chemical Industry Co. Ltd. (Tokyo, Japan). Avidin-biotin horseradish peroxidase (HRP) complex reagent, biotinylated secondary antibodies, diaminobenzidine tetrahydrochloride, and antifade reagent were obtained from Vector Laboratories (Burlingame, CA, USA). The following primary antibodies were used in this study: anti-p-AMP kinase protein (p-AMPK), anti-total form of AMPK, anti-interleukin (IL)-6, anti-p-mammalian target of rapamycin (p-mTOR), anti-total form of mTOR, anti-tyrosine hydroxylase (TH), anti-p-α-syn (Ser129), and anti-α-syn (Cell Signaling Technology, Inc., Danvers, MA, USA); anti- inducible nitric oxide synthase (iNOS) (BD Bioscience, San Jose, CA, USA); anti-β-actin and anti-glial fibrillary acidic protein (GFAP) (Sigma-Aldrich); anti-ionized calcium-binding adapter molecule 1 (Iba-1) (Wako, Osaka, Japan); and anti-tumor necrosis factor (TNF)-α (Santa Cruz Biotechnology, Dallas, TX, USA). HRP-conjugated secondary antibodies were purchased from Bio-Rad (Hercules, CA, USA).

2.2. Animals

Adult male C57BL/6 mice (7-week-old) were purchased from Orient Bio, Inc. (Seongnam, South Korea), a branch of Charles River Laboratories. Mice were maintained at 21°C under a 12-h light:dark cycle and had ad libitum access to water and rodent chow. Every effort was made to minimize animal suffering. All experiments were performed in accordance with the guidelines of the National Institutes of Health and Ewha Womans University for the care and use of laboratory animals. The study was approved by the Institutional Animal Care and Use Committee of the Medical School of Ewha Womans University (#EWHA MEDIACUC 21–012-t). The study was carried out in compliance with the ARRIVE guidelines.

2.3. MPTP administration and experimental procedure

Mice were randomly divided into the following six groups: CON, control; M/P, MPTP+probenecid; M/P + GTS, M/P + GTS-21; M/P + PNU, M/P + PNU-282987; GTS and PNU (each group N = 30–35). MPTP was administered intraperitoneally (i.p.) for five consecutive days. In brief, mice were administered MPTP (25 mg/kg i.p.) twice a day at a 6-h interval on days 1 and 2 and once a day on days 3–5. Mice were treated with probenecid (250 mg/kg/d, subcutaneously) 30 min before MPTP injection to promote the prolonged neuronal retention of MPTP. Thereafter, GTS (1 mg/kg/d for 3 d and 2 mg/kg/d for 7 d) and PNU (2 mg/kg/d for 3 d and 5 mg/kg/d for 7 d) were i.p. injected for 3 weeks, followed by the subjection of animals to behavioral tests 2 and 3 d, and euthanization 4 d after the last drug treatment. For antagonistic experiments using MLA, the protocol for MPTP and GTS administration and euthanasia were identical to the above experimental procedure. MLA was injected 1 h before the GTS treatment (0.5 mg/kg/d, 7 d)

2.4. Behavioral tests

An accelerated rotarod test was performed to assess motor coordination. Five days before drug treatment, all mice were trained on the rotarod (4–13 rpm) until they remained on the apparatus for 300 s without falling. The rotarod was accelerated from 4 to 40 rpm over a 300-s period. Mice were subjected to three trials at 15-min intervals. The retention time on the rods in each trial was recorded. A pole test (50 cm height, 0.5 cm diameter) was used to evaluate akinesia. Mice were subjected to three trials at 15-min intervals. The time required for each mouse to descend the pole was recorded. For the beam walking test, each mouse was allowed to traverse a round wooden beam 0.7 cm in diameter and 70 cm in length elevated 70 cm from the ground. During the time in which the mouse traversed, the corresponding scores were recorded. The test was conducted three times, and walking behavior and gait performance were used to calculate the score (0–4 points). The average score of three consecutive trials was calculated as follows: 0 points, the mouse could not grip the wooden beam or sit on the wooden beam and fell directly; 1 point, the mouse could grip the wooden beam or sit on the wooden beam, could not move, but could stay on for 30 s; 2 points, the mouse maintained balance on the wooden beam, could not cross the beam, but could stay on for 30 s; 3 points, the

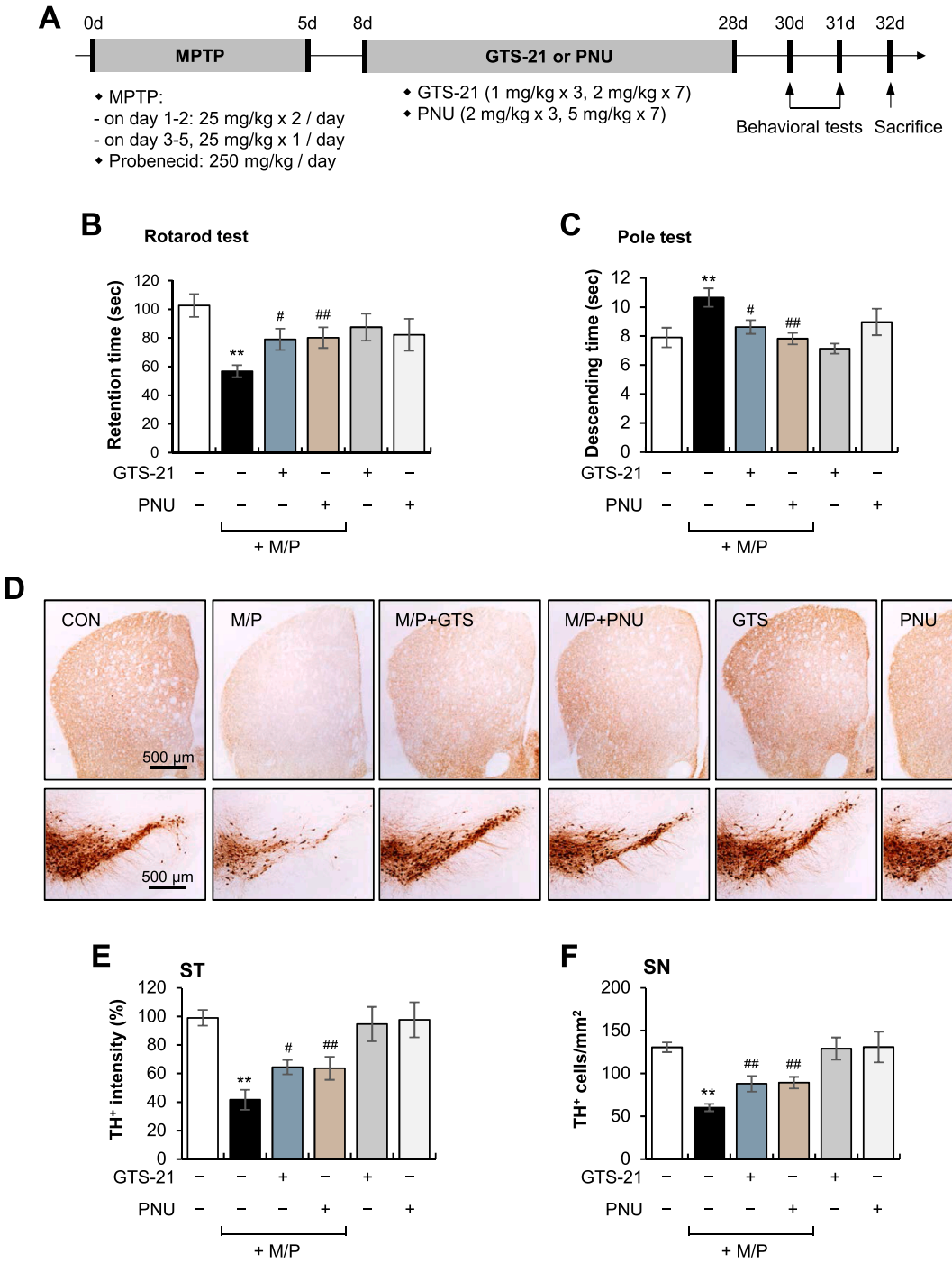
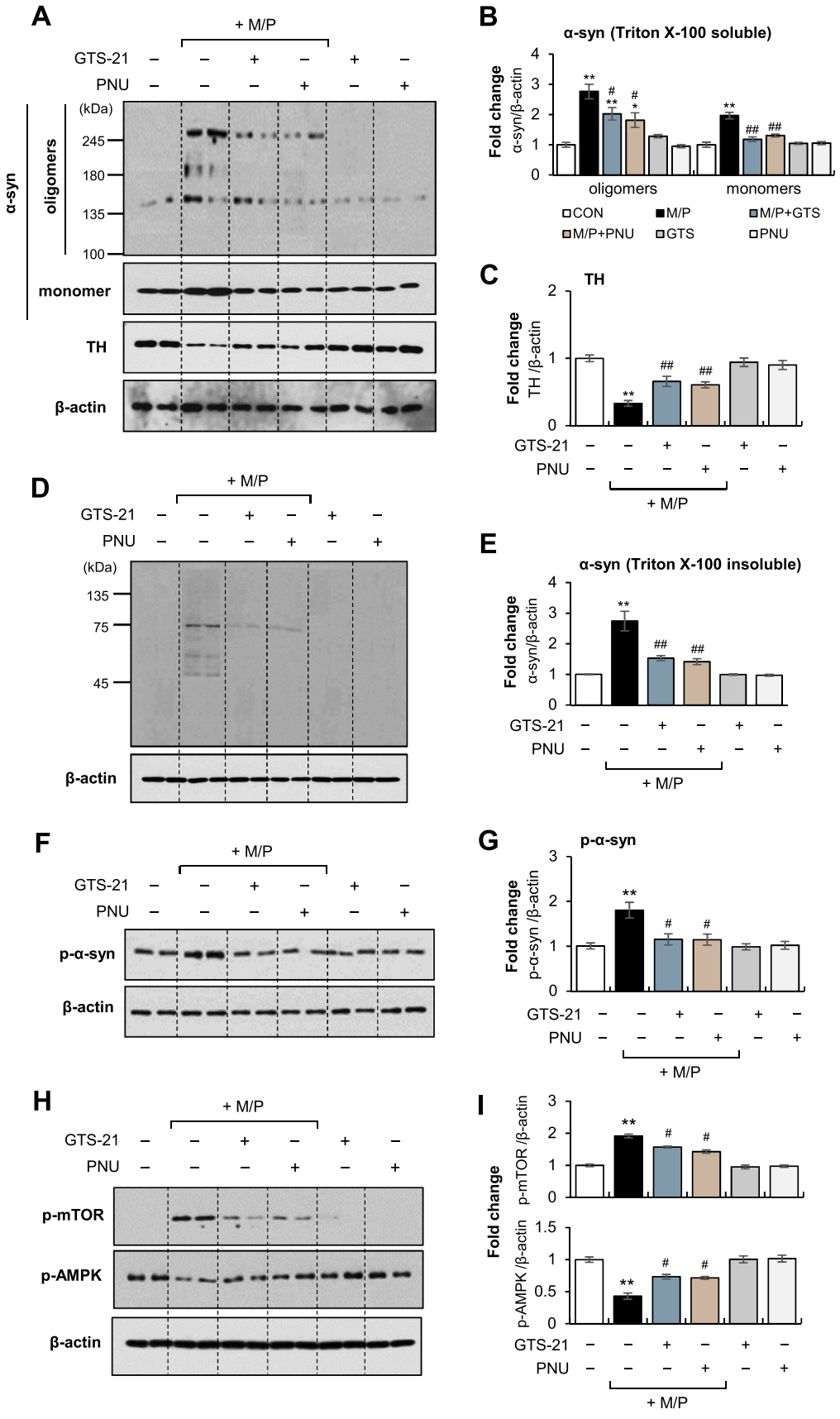


Fig. 1. GTS-21 and PNU administration restored impaired motor performance and alleviated nigrostriatal dopaminergic degeneration in subacute MPTP mice. A. Schematic of experimental procedure. Mice were injected intrapenitoneally with MPTP for 5 consecutive days at 25–50 mg/kg/d (on days 1–2: 25 mg/kg × 2/d; on days 3–5: 25 mg/kg × 1/d). Probenecid was preinjected subcutaneously 1 h before MPTP administration (250 mg/kg/d) to prevent MPTP excretion from the body. GTS (1 mg/kg/d × 3 d and subsequently 2 mg/kg/d × 7 d) and PNU (2 mg/kg/d × 3 d and subsequently 5 mg/kg/d × 7 d) were administrated intrapenitonally. Two days after the last exposure to drugs, behavioral, histological, and biochemical analyses were conducted. **B.** GTS-21 and PNU administration enhanced the retention time in the accelerating rotarod test in MPTP mice (each group N = 8–12). **C.** GTS-21 and PNU administration reduced the descending time in the pole test in MPTP mice (each group N = 8–12). **D.** A photomicrograph showing TH^+ fibers in the striatum and TH^+ cells in SNpc regions. **E.** GTS-21 and PNU administration increased the TH^+ intensities in the striatum of MPTP mice (each group N = 6–7). **F.** GTS-21 and PNU administration increased the number of TH^+ cells in the SNpc of MPTP mice (each group N = 6–7). Data are expressed as the mean ± SEM. * $^{*}p < 0.01$ vs. CON; $^{\#}p < 0.05$ and $^{\#\#}p < 0.01$ vs. M/P.

mouse could walk from one end of the beam to the other, but footfall occurred; and 4 points, the mouse could freely move from one end of the beam to the other end of the beam [33].

2.5. Histological analysis

Brain sections were obtained as previously described (striatum: every six sections/brain; substantia nigra (SN): every three sections/brain) [34]. Endogenous peroxidation was blocked with 3 % hydrogen



(caption on next page)

Fig. 2. GTS-21 and PNU administration reduced α-syn oligomerization and p-α-syn levels in the SN area of subacute MPTP mice. A. GTS-21 and PNU administration reduced the levels of α-syn oligomer and monomer species and those of TH protein in the SN of MPTP mice (each group N = 4–6). **B.** Diagram showing the quantification of the levels of α-syn oligomer and monomer species. **C.** Diagram showing the quantification of TH levels. **D.** GTS-21 and PNU administration reduces the levels of Triton X-100 insoluble α-syn oligomers in the SN of MPTP mice (each group N = 4). **E.** Diagram presenting the quantification of Triton X-100 insoluble α-syn oligomer levels. **F.** GTS-21 and PNU administration decreased p-α-syn levels in the SN of MPTP mice (each group N = 4–6). **G.** Diagram showing the quantification of p-α-syn levels. **H.** GTS-21 and PNU administration decreases p-mTOR levels and increases p-AMPK levels in the SN of MPTP mice (each group, N = 4). **I.** Diagram showing the quantification of p-mTOR and p-AMPK levels. Data are expressed as the mean ± SEM. * $^{*}p < 0.01$ vs. CON; $^{\#}p < 0.05$ and $^{\#\#}p < 0.01$ vs. M/P.

peroxide, while nonspecific binding was blocked with 4 % bovine serum albumin. The sections were incubated overnight with primary antibodies and then with biotinylated secondary antibodies for 1 h at 25°C on the following day. The sections were subsequently incubated with an avidin-biotin-HRP complex reagent solution for 1.5 h, followed by a peroxidase reaction using diaminobenzidine tetrahydrochloride. For double immunofluorescence, nonspecific binding was blocked, and the sections were incubated with primary antibodies, followed by fluorochrome-conjugated secondary antibodies. For thioflavin-S (Thio-S) staining, sections were stained with thioflavin-S (Thio-S) for 8 min, rinsed twice with 50 % ethanol for 5 min, and then washed with phosphate-buffered saline. Digital images of immunohistochemical and immunofluorescence staining were captured using a Leica DM750 microscope (Leica Microsystems, North Deerfield, IL, USA). Quantification was performed using the ImageJ software (NIH, Bethesda, MD, USA).

2.6. Western blotting analysis

Tissues collected from the striatum and SN of the brain and distal colon (1 cm specimen; 3 cm from the anal verge) were homogenized in ice-cold lysis buffer. Subsequently, the samples were vortexed vigorously at 10-min intervals and then incubated for 30 min at 4°C. The samples were then centrifuged at 10000 × *g* for 15 min and the supernatant was collected (S1). The pellet was resuspended in lysis buffer, and following a repeat centrifugation, the supernatant (S2) was obtained. These protein extracts (S1 and S2) represented the Triton X-100-soluble fraction. For the Triton X-100-insoluble fraction, the final pellet was sonicated in 2 % SDS lysis buffer (50 mM Tris-HCl, pH 6.8, 2 % SDS, 5 % glycerol, 1 % 2-ME). Protein samples (50–100 μg: Triton X-100-soluble; equal volume: Triton X-100-insoluble) were separated using SDS-PAGE, transferred to a nitrocellulose membrane, and incubated with primary antibodies according to the manufacturer's instructions. The membranes were thoroughly washed with TBST and incubated with HRP-conjugated secondary antibodies. Subsequently, the blots were developed using an enhanced chemiluminescence detection kit (Thermo Fisher Scientific, Waltham, MA, USA). The density of specific target bands was normalized against that of β-actin for quantification using the ImageJ software.

2.7. Statistical analysis

Statistical analyses were performed using SPSS for Windows (version 18.0; SPSS Inc., Chicago, IL, USA). Differences among groups were analyzed using one-way analysis of variance. Post-hoc comparisons were conducted using the Tukey's test. All values are presented as the mean ± standard error of the mean (SEM). Differences were considered statistically significant at $p < 0.05$.

3. Results

3.1. GTS-21 and PNU improved motor function and reduced nigrostriatal dopaminergic degeneration in subacute MPTP mice

To examine the effects of GTS-21 and PNU on the PD mouse model, we injected mice with MPTP for five consecutive days, followed by GTS and PNU administration for 3 weeks (Fig. 1A). We used the accelerating-speed rotarod and pole tests to assess motor coordination and akinesia, which are two critical motor properties of the PD mouse model. GTS-21 and PNU rescued the MPTP-induced decline in retention time on the rod as measured in the rotarod test (Fig. 1B; $F_{5,\ 57} = 3.86$, $p < 0.01$) and the MPTP-induced elevation in descending time in the pole test (Fig. 1C; $F_{5,\ 57} = 4.70$, $p < 0.01$). This finding suggested that GTS-21 and PNU promoted behavioral recovery from motor impairment in our experimental paradigm. Consistent with the behavioral data, GTS-21 and PNU resulted in restoration of nigrostriatal degeneration against MPTP neurotoxicity, as indicated by the recovery in the number of TH^+ fibers in the striatum (Fig. 1D,E; $F_{5,\ 39} = 8.01$, $p < 0.01$) and TH^+ cells in the SN (Fig. 1D,F; $F_{5,\ 39} = 9.11$, $p < 0.01$).

3.2. GTS-21 and PNU reduced α-syn oligomerization and p-α-syn levels in the SN area of subacute MPTP mice

As abnormal α-syn protein oligomerization/aggregation and phosphorylation play a crucial role in PD progression, we measured the levels of α-syn oligomer and monomer species using immunoblot analysis. We observed a considerable decrease in the levels of α-syn oligomer and monomer species in the SN area of MPTP-treated mice following GTS-21 and PNU administration (Fig. 2A,B; for oligomers $F_{5,\ 28} = 10.86$, $p < 0.01$; for monomer $F_{5,\ 28} = 21.70$, $p < 0.01$). Conversely, TH levels were significantly increased in the SN area of MPTP-treated mice after GTS-21 and PNU administration (Fig. 2A,C; $F_{5,\ 28} = 16.88$, $p < 0.01$), corresponding well to histological results. Triton X-100 fractionation performed to demonstrate α-syn aggregation revealed that the α-syn species resistant to Triton X-100 solubility were elevated in MPTP mice compared with controls, but were decreased by treatment with GTS-21 and PNU (Fig. 2D,E; $F_{5,\ 23} = 23.07$, $p < 0.01$). Moreover, p-α-syn levels decreased in response to GTS-21 and PNU administration in the SN area of MPTP-treated mice (Fig. 2F,G; $F_{5,\ 28} = 6.48$, $p < 0.01$). Furthermore, autophagy-regulating molecules, including mTOR and AMPK, were detected in the SN region. MPTP increased mTOR phosphorylation, which was reversed by GTS-21 and PNU treatment (Fig. 2H,I; $F_{5,\ 23} = 72.58$, $p < 0.01$). Conversely, MPTP decreased AMPK phosphorylation, which was restored by GTS-21 and PNU treatment (Fig. 2H,I; $F_{5,\ 23} = 28.99$, $p < 0.01$). We found that total AMPK levels did not differ across groups. On the contrary, total mTOR levels were considerably raised in the MPTP group, which was reversed by GTS-21 and PNU, implying that higher mTOR phosphorylation may be attributable to increased mTOR expression (Supplementary Fig. 1). These results indicate that GTS-21- and PNU-stimulated α7nAchR activation reduced pathogenic α-syn production under MPTP-induced noxious conditions, in which the AMPK-mTOR autophagy pathways are involved.

3.3. GTS-21 and PNU reduced the number of TH^+/thio-S^+ cells and p-α-syn^+/thio-S^+ particles in the SN area of subacute MPTP mice

Using double immunofluorescence approach, we validated the transition of α-syn to its pathogenic form in our experimental paradigm. Both the Thio-S^+ and Thio-S^+/TH^+ areas were profoundly enhanced under MPTP exposure. Conversely, GTS-21 and PNU administration reversed this effect in the SN area of MPTP mice (Fig. 3A-C; for Thio-S^+ area, $F_{5,\ 27} = 12.87$, $p < 0.01$; for Thio-S^+/TH^+ area, $F_{5,\ 32} = 15.24$, $p < 0.01$). Furthermore, both the p-α-syn^+ and p-α-syn^+/Thio-S^+ areas corresponded well to the Thio-S^+ and Thio-S^+/TH^+ areas (Fig. 3D-F; for p-α-syn^+ area, $F_{5,\ 42} = 12.40$, $p < 0.01$; for p-α-syn^+/Thio-S^+ area, $F_{5,\ 42}$

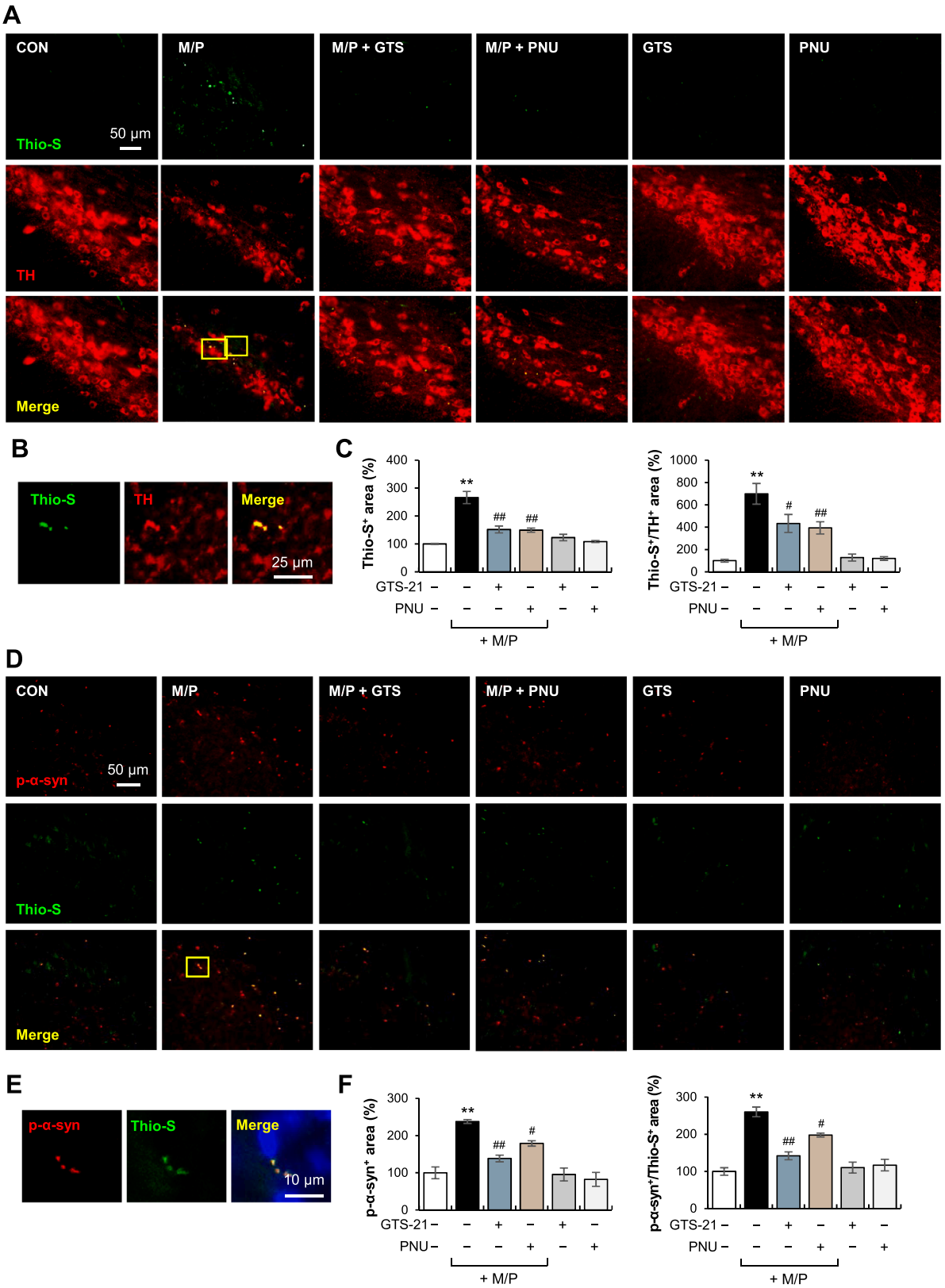


Fig. 3. GTS-21 and PNU administration reduced the number of TH$^+$/thio-S$^+$ cells and p-α-syn$^+$/thio-S$^+$ particles in the SN area of subacute MPTP mice. A. A photomicrograph showing Thio-S$^+$/TH$^+$ particles in SNpc regions. GTS and PNU administration decreased the Thio-S$^+$/TH$^+$ area in the SN of MPTP mice (each group N = 5–7). The yellow square indicates the precise location of the high magnification. **B.** High magnification of the area of Thio-S$^+$/TH$^+$ fluorescence staining. **C.** Diagram showing the quantification of the Thio-S$^+$ and Thio-S$^+$/TH$^+$ areas. **D.** A photomicrograph showing p-α-syn$^+$/Thio-S$^+$ particles in SNpc regions. GTS and PNU administration decreased the p-α-syn$^+$/Thio-S$^+$ area in the SN of MPTP mice (each group N = 5–8). The yellow square indicates the precise location of the high magnification. **E.** High magnification of the area of p-α-syn$^+$/Thio-S$^+$ fluorescence staining. **F.** Diagram showing the quantification of the p-α-syn$^+$ and p-α-syn$^+$/Thio-S$^+$ areas. Data are expressed as the mean ± SEM. * *$p < 0.01$ vs. CON; $^{\#}p < 0.05$ and $^{\#\#}p < 0.01$ vs. M/P.

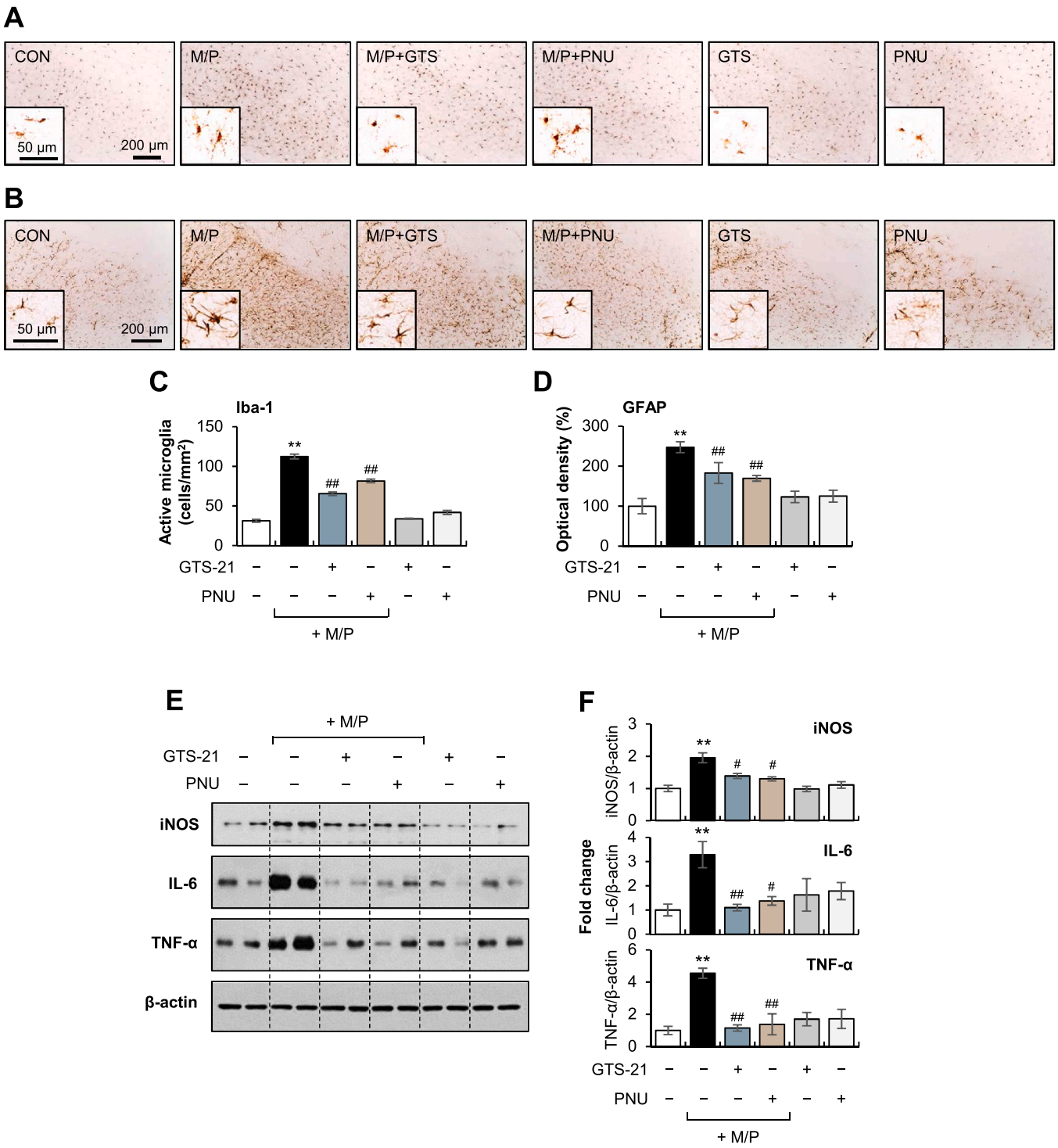
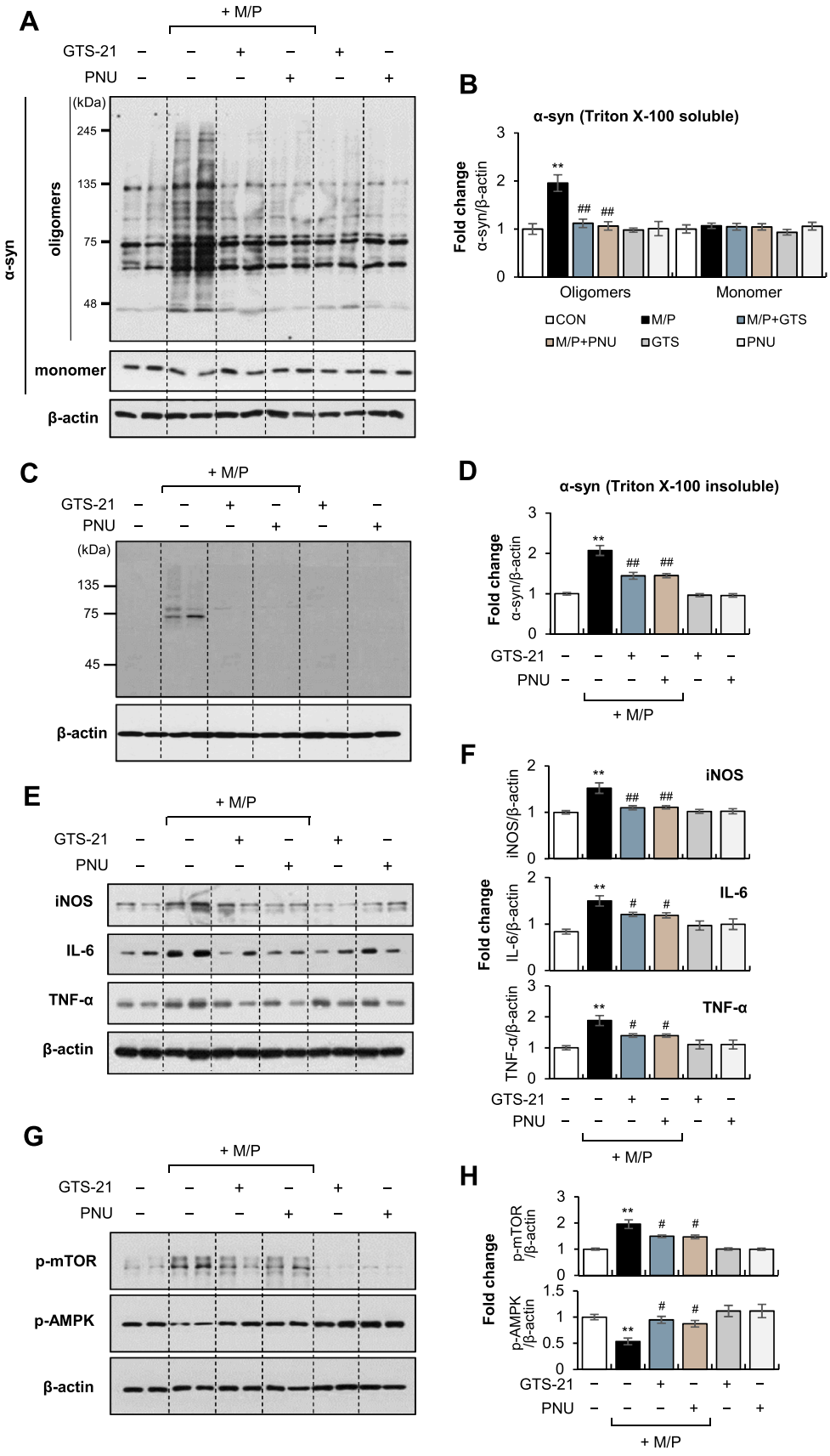


Fig. 4. GTS-21 and PNU administration suppressed the activation of microglia and astrocytes, and the expression of proinflammatory markers in the SN area of subacute MPTP mice. A. A photomicrograph showing Iba-1$^+$ cells in SNpc regions. GTS and PNU administration decreased the number of ameboid Iba-1$^+$ cells in the SN of MPTP mice (each group N = 4–6). **B.** A photomicrograph showing GFAP$^+$ cells in SNpc regions. GTS and PNU administration decreased GFAP$^+$ intensities in the SN of MPTP mice (each group N = 4–6).
C. Diagram showing the quantification of ameboid Iba-1$^+$ cells. **D.** Diagram showing the quantification of GFAP$^+$ intensities. **E.** GTS and PNU administration inhibited the expression of proinflammatory markers in the SN area of MPTP mice (each group N = 4–6). **F.** Diagram showing the quantification of iNOS, IL-6, and TNF-α. Data are expressed as the mean ± SEM. $^{**}p < 0.01$ vs. CON; $^{\#}p < 0.05$ and $^{\#\#}p < 0.01$ vs. M/P.

=10.26, $p < 0.01$). These results indicated that GTS-21 and PNU administration reduced the elevated α-syn aggregation in dopaminergic neurons in the SN area of MPTP mice.

3.4. GTS-21 and PNU suppressed microglia activation and expression of proinflammatory markers in the SN area of subacute MPTP mice

As neuroinflammation is a major component of PD progression, we assessed the microglia and astrocyte phenotypes by



(caption on next page)

Fig. 5. GTS-21 and PNU administration reduced α-syn oligomerization and expression of proinflammatory markers in the distal colon area of subacute MPTP mice. A. GTS and PNU administration reduced the number of α-syn oligomer species in the distal colon area of MPTP mice (each group N = 5–7). **B.** Diagram showing the quantification of α-syn oligomer and monomer species. **C.** GTS-21 and PNU administration reduces the levels of Triton X-100 insoluble α-syn oligomers in the distal colon region of MPTP mice (each group N = 4). **D.** Diagram presenting the quantification of Triton X-100 insoluble α-syn oligomer levels. **E.** GTS and PNU administration reduced iNOS, IL-6, and TNF-α levels in the colon area of MPTP mice (each group N = 5–7). **F.** Diagram showing the quantification of iNOS, IL-6, and TNF-α. **G.** GTS-21 and PNU administration decreases p-mTOR levels, and increases p-AMPK levels in the distal colon region of MPTP mice (each group N = 4). **H.** Diagram showing the quantification of p-mTOR and p-AMPK levels.Data are expressed as the mean ± SEM. * *$p < 0.01$ vs. CON; $^{\#}p < 0.05$ and $^{\#\#}p < 0.01$ vs. M/P.

immunohistochemistry using Iba-1 and GFAP antibodies. GTS-21 and PNU administration markedly reduced the number of active microglia and reactive astrocytes in the SN of MPTP mice (Fig. 4A,C; $F_{5,\ 24} = 60.54$, $p < 0.01$; Fig. 4B,D; $F_{5,\ 24} = 6.07$, $p < 0.01$). In addition, GTS-21 and PNU administration inhibited the expression of proinflammatory markers, such as TNF-α, IL-6, and iNOS in the SN region of MPTP mice (Fig. 4E,F; for iNOS, $F_{5,\ 29} = 12.15$, $p < 0.01$; for IL-6, $F_{5,\ 18} = 4.27$, $p < 0.01$; for TNF-α, $F_{5,\ 21} = 7.51$, $p < 0.01$). These results indicated that the GTS-21- and PNU-induced α7nAchR stimulation exerted anti-inflammatory effects under sustained MPTP-induced neuroinflammation.

3.5. GTS-21 and PNU reduced α-syn oligomerization and expression of proinflammatory markers in the distal colon area of subacute MPTP mice

In the distal colon enriched in α7nAchR, GTS-21 and PNU administration resulted in a considerable reduction in the levels of α-syn oligomer species, but not that of monomer (Fig. 5A,B; for oligomers $F_{5,\ 32} = 10.95$, $p < 0.01$; for monomer $F_{5,\ 32} = 0.51$, $p > 0.05$). In Triton X-100 fractionation, α-syn species resistant to Triton X-100 solubility were elevated in MPTP mice compared with controls but were decreased by GTS-21 and PNU treatment (Fig. 5C,D; $F_{5,\ 23} = 38.81$, $p < 0.01$). Furthermore, GTS-21 and PNU administration dampened the expression of proinflammatory mediators in the distal colon of MPTP mice (Fig. 5E, F; for iNOS, $F_{5,\ 32} = 10.07$, $p < 0.01$; for IL-6, $F_{5,\ 18} = 8.02$, $p < 0.01$; for TNF-α, $F_{5,\ 21} = 8.19$, $p < 0.01$). Similar to the brain tissue, GTS-21 and PNU suppressed p-mTOR and increased p-AMPK (Fig. 5G,H; for p-mTOR, $F_{5,\ 23} = 23.08$, $p < 0.01$; for p-AMPK, $F_{5,\ 23} = 6.59$, $p < 0.01$).

While total AMPK levels did not differ across groups, total mTOR levels were significantly elevated in the MPTP group, which was reversed by GTS-21 and PNU, similar to the brain (Supplementary Fig. 1). These results implied that GTS-21- and PNU-stimulated α7nAchR activation induced α-syn degradation and anti-inflammatory capacity in the gastrointestinal system, possibly through the modulation of the AMPK-mTOR autophagy pathway.

3.6. MLA pretreatment abolished the GTS-21-elicited restoration of impaired motor performance and nigrostriatal dopaminergic degeneration in subacute MPTP mice

To reconfirm the specific effect of α7nAchR-stimulated behavioral improvement, we pretreated mice with a α7 nAchR antagonist, MLA, and assessed their motor performance (Fig. 6A). In the rotarod test, the GTS-21-elicited increase in retention time on the rod was not significantly reversed by MLA pretreatment in MPTP mice (Fig. 6B; $F_{3,\ 26} = 2.60$, $p > 0.05$). On the contrary, in the beam walking test, another behavioral test measuring motor coordination and balance in rodents, the GTS-21-induced increase in beam walking score and decrease in footfall frequency were reversed by MLA pretreatment in MPTP mice (Fig. 6C,D; for beam walking score $F_{3,\ 26} = 6.01$, $p < 0.01$; for footfall frequency $F_{3,\ 26} = 6.18$, $p < 0.01$). Pretreatment with MLA abolished the GTS-21-induced increase in TH^+ intensity in the striatum and number of TH^+ cells in the SN (Fig. 6E-G; for striatum $F_{3,\ 28} = 47.3$, $p < 0.01$; for SN $F_{3,\ 20} = 12.43$, $p < 0.01$). These results indicated that the GTS-21-elicited recovery of motor performance and nigrostriatal dopaminergic neurotransmission is dependent on α7nAchR activity in the brain.

3.7. MLA pretreatment abolished the GTS-21-elicited decrease in the number of p-α-syn$^+$/thio-S$^+$ particles and α-syn oligomerization in the SN area of subacute MPTP mice

In the α7nAchR antagonistic experiments linked to α-syn pathology, the GTS-21-induced decrease in p-α-syn^+ and p-α-syn^+/Thio-S^+ areas was reversed by MLA pretreatment in MPTP mice (Fig. 7A-C; for p-α-syn^+ $F_{3,\ 23} = 21.51$, $p < 0.01$; for p-α-syn^+/Thio-S^+ $F_{3,\ 23} = 32.02$, $p < 0.01$). The immunoblot data corresponded well to histological results. Thus, the GTS-21-mediated reduction in α-syn oligomer and monomer species was reversed by MLA pretreatment in MPTP mice (Fig. 7D,E; for oligomers $F_{3,\ 11} = 13.44$, $p < 0.01$; for monomer $F_{3,\ 11} = 13.84$, $p < 0.01$). These results implied that the GTS-21-induced reduction in pathogenic α-syn formation relied on α7nAchR activity in the brain.

3.8. MLA pretreatment abolished the GTS-21-elicited reduction in microglial activation and expression of proinflammatory markers in the SN area of subacute MPTP mice

In the α7nAchR antagonistic experiments linked to inflammatory responses, the GTS-21-induced decrease in active microglia population was inversely enhanced by MLA pretreatment in MPTP mice (Fig. 8A,B; $F_{3,\ 20} = 24.95$, $p < 0.01$). In addition, the GTS-21-induced decrease in the expression of proinflammatory mediators was also reversed by MLA pretreatment in the SN region of MPTP mice (Fig. 8C,D; for iNOS, $F_{3,\ 15} = 15.68$, $p < 0.01$; for IL-6, $F_{5,\ 18} = 22.22$, $p < 0.01$; for TNF-α, $F_{5,\ 21} = 7.40$, $p < 0.01$). These results implied that the GTS-21-induced decrease in the expression of proinflammatory mediators was dependent on α7nAchR activity in the brain.

3.9. MLA pretreatment abolished the GTS-21-elicited reduction in α-syn oligomerization and expression of proinflammatory markers in the distal colon area of subacute MPTP mice

In the α7nAchR antagonistic experiments linked to α-syn pathology and inflammation in the gut, pretreatment with MLA abolished the effect of GTS-21 on α-syn pathology (Fig. 9A,B; for oligomers $F_{3,\ 12} = 45.53$, $p < 0.01$; for monomer $F_{3,\ 12} = 19.13$, $p < 0.01$) and inflammation in the gut (Fig. 9C,D; for iNOS, $F_{3,\ 12} = 13.40$, $p < 0.01$; for IL-6, $F_{3,\ 12} = 51.10$, $p < 0.01$; for TNF-α, $F_{5,\ 12} = 8.53$, $p < 0.01$). We found that the ability of GTS-21 to reduce α-syn pathology and inflammation relied on α7nAchR activity in the gut, comparable to the changes observed in the brain.

4. Discussion

This study demonstrated that α7nAchR agonists, GTS-21 and PNU, ameliorated the nigrostriatal dopaminergic degeneration and induced behavioral recovery in the subacute MPTP mouse model of PD. Moreover, GTS-21 and PNU inhibited α-syn oligomerization and aggregation in the SN region and distal colon segment of subacute MPTP-treated mice. Apart from the positive changes in α-syn pathology, GTS-21 and PNU profoundly improved MPTP-induced inflammation in both the brain and gut tissues. On the contrary, pretreatment with the α7nAchR antagonist, MLA, abrogated the beneficial effect of GTS-21 in the SN and distal colon regions. These results suggested that activating α7nAchR may improve PD symptoms by affecting both the brain and gut. Fig. 10

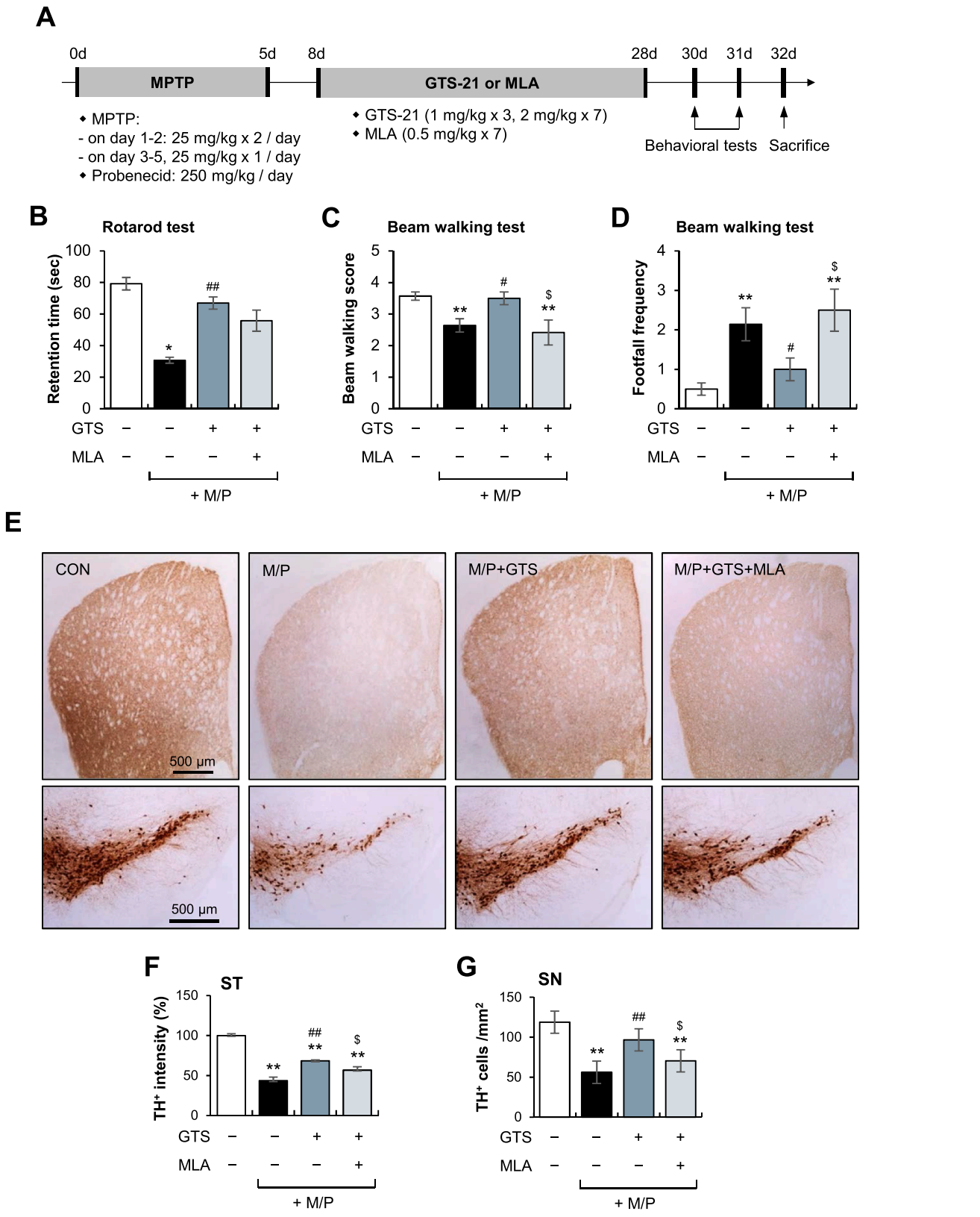


Fig. 6. MLA pretreatment abolished the GTS-21-elicited restoration of impaired motor performance and nigrostriatal dopaminergic degeneration in subacute MPTP mice. A. Schematic of experimental procedure. The protocol for MPTP and GTS administration and euthanasia was identical to that in the previous experimental procedure (Fig. 1A). MLA was injected 1 h before GTS treatment (0.5 mg/kg/d, 7 d). **B.** MLA pretreatment did not significantly reverse the GTS-induced increase in retention time in the rotarod test (each group N = 5–8). **C-D.** MLA pretreatment reversed the GTS-induced improvement in the beam walking score (C) and footfall frequency (D) in the beam walking test (each group N = 5–8). **E.** MLA pretreatment reversed the GTS-induced increase in the number of TH^+ fibers in the striatum and TH^+ cells in SNpc regions in MPTP mice (each group N = 5–8). **F-G.** Diagram showing the quantification of TH^+ intensities (F) and TH^+ cells (G). Data are expressed as the mean ± SEM. * $^*p < 0.01$ vs. CON; $^{\#}p < 0.05$ and $^{\#\#}p < 0.01$ vs. M/P. $^{\$}p < 0.05$ vs. M/P + GTS.

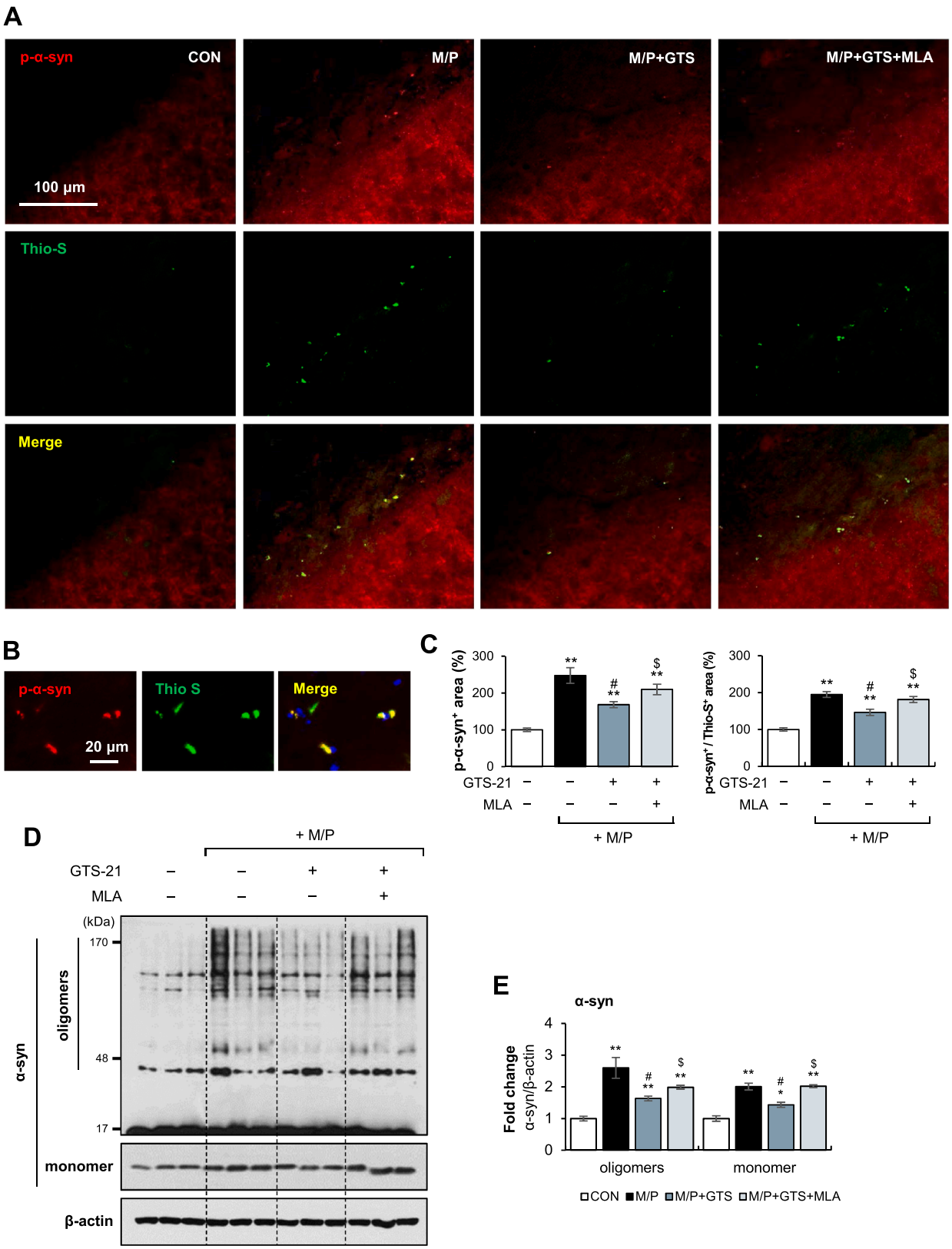


Fig. 7. MLA pretreatment abolished the GTS-21-elicited decrease in p-α-syn$^+$/thio-S$^+$ particles and α-syn oligomerization in the SN area of subacute MPTP mice. A. Photomicrograph showing p-α-syn$^+$/Thio-S$^+$ particles in SNpc regions. MLA pretreatment reversed the GTS-induced decrease in p-α-syn$^+$ and p-α-syn$^+$/Thio-S$^+$ areas (each group N = 4–6). **B.** High magnification of the area of p-α-syn$^+$/Thio-S$^+$ fluorescence staining. **C.** Diagram showing the quantification of p-α-syn$^+$ and p-α-syn$^+$/Thio-S$^+$ areas. **D.** MLA pretreatment abolished the GTS-induced suppression of α-syn oligomerization (each group N = 4–6). **E.** Diagram showing the quantification of the levels of α-syn oligomer and monomer species. Data are expressed as the mean ± SEM. * $^*p < 0.01$ vs. CON; $^{\#}p < 0.05$ vs. M/P; $^{\$}p < 0.05$ vs. M/P + GTS.

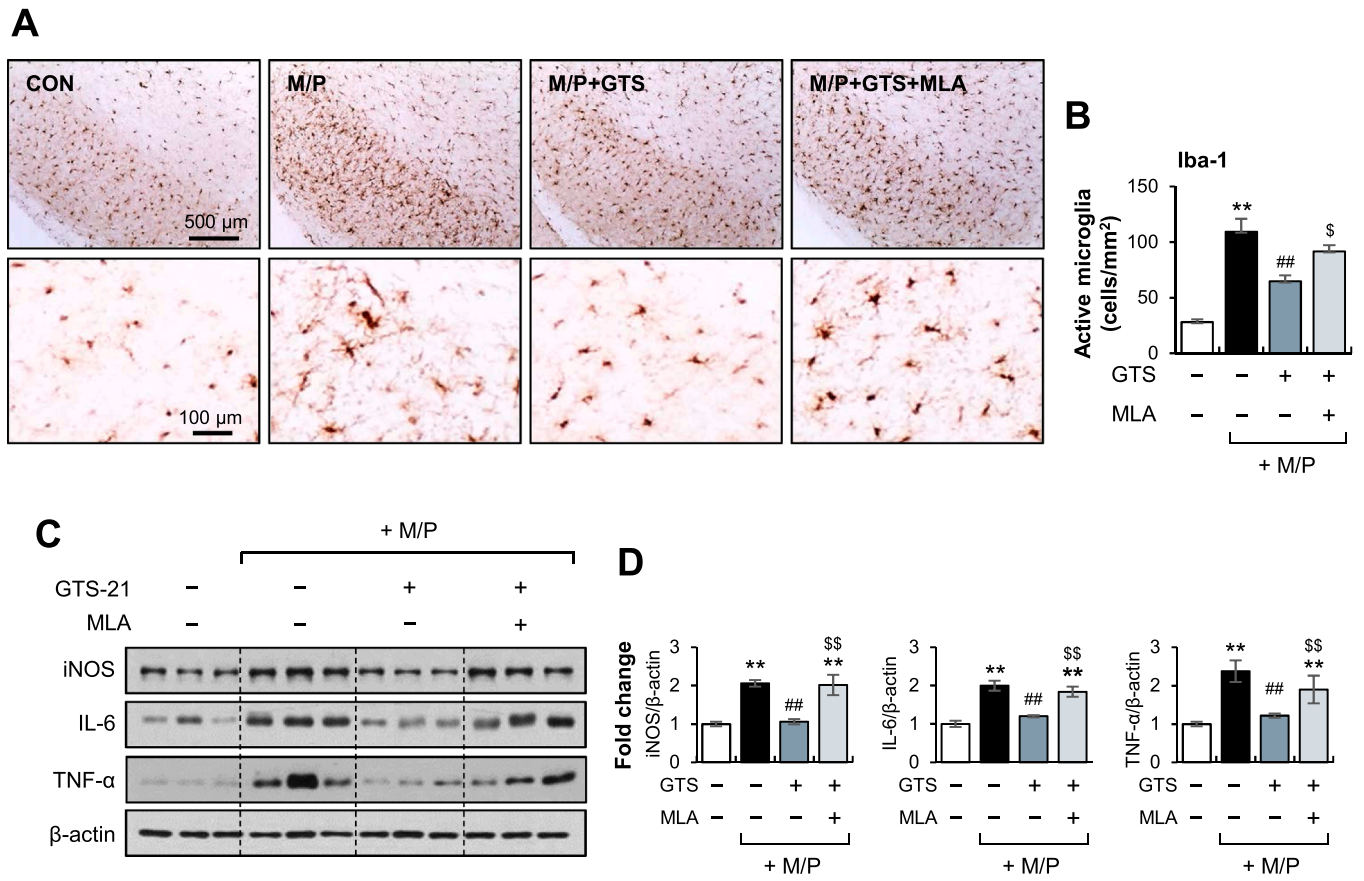


Fig. 8. MLA pretreatment abolished the GTS-21-elicited inhibition in microglial activation and expression of proinflammatory markers in the SN area of subacute MPTP mice. A. Photomicrograph showing ameboid Iba-1$^+$ cells in SNpc regions. MLA pretreatment reversed the GTS-induced decrease in the number of ameboid Iba-1$^+$ cells (each group N = 4–6). **B.** Diagram showing the quantification of ameboid Iba-1$^+$ cells. **C.** MLA pretreatment abolished the GTS-induced decrease in the levels of iNOS, IL-6, and TNF-α in the SN area of MPTP mice (each group N = 4–6). **D.** Diagram showing the quantification of the levels of iNOS, IL-6, and TNF-α. Data are expressed as the mean ± SEM. * *$p < 0.01$ vs. CON; $^{\#\#}p < 0.01$ vs. M/P; $^{\$}p < 0.05$ vs. M/P + GTS; $^{\$\$}p < 0.01$ vs. M/P + GTS.

summarizes the effects of α7nAchR agonists on the brain and gut in the PD mouse model.

PD belongs to α-synucleinopathies, which include dementia with Lewy bodies and multiple system atrophy. The pathophysiology of insoluble amyloid aggregates is mostly attributed to the deposition of α-syn, which eventually results in persistent inflammation and the death of dopaminergic cells [35]. Several studies have suggested the spread of α-syn pathology throughout the gut-brain axis. Clinical and epidemiological studies have shown that pathogenic α-syn species deposit in peripheral tissues, including the gastrointestinal tract, before causing motor impairment [15]. Exogenous α-syn fibrils implanted into the guts of mice have been shown to spread to their brains [36–38]. In mice, vagotomy reduced the distribution of gut-injected α-syn fibrils to the brain [38,39]. Therefore, improving α-syn pathology by targeting both the brain and gut is necessary for the prevention and treatment of PD. In this study, we found that α7nAchR agonists reduced α-syn aggregation in the brain and gut. However, to establish a clear link between the brain-gut axis and α7nAchR activation, a model of α-syn fibril conveyance from the gut to the brain and vagotomy is needed in the near future.

Several studies have demonstrated that nicotine alters α-syn pathophysiology. Nicotine, a nonselective nAchR agonist, was reported to suppress α-syn fibrillation, destabilize preformed α-syn fibrils, and stabilize soluble α-syn oligomers in vitro [40,41]. Nicotine was reported to activate the D3R-nAchR complex and inhibit α-syn deposition in human iPSC-derived dopaminergic neuron and primary mesencephalic cultures [42]. Furthermore, PNU and nicotine reduced α-syn accumulation in cells treated with or overexpressing α-syn in a dose-dependent manner [22]. In that study, α7nAchR deficiency increased the number of α-syn deposits and worsened dopaminergic degeneration [22]. These results were consistent with those in the present study demonstrating that the activation of α7nAchR by GTS-21 and PNU significantly reduced α-syn oligomerization and aggregation in the SN and distal colon of subacute MPTP animals, which was reversed by the α7nAchR antagonist. Consequently, our results, in conjunction with those of previous studies, have suggested a close correlation between α7nAchR and pathogenic α-syn production. The activation of α7 nAchR may facilitate the degradation and elimination of α-syn.

The brain is equipped with homeostatic systems that eliminate neurotoxic protein oligomers and aggregates. These systems include the ubiquitin-proteasome system, chaperon-mediated autophagy, and autophagy-lysosomal pathway [43–45]. The autophagy-lysosomal route destroys the pathogenic form of α-syn more effectively than the ubiquitin-proteasome system under normal conditions [46,47]. A study found that α7nAchR loss affected autophagy flux in an inflammatory bowel disease animal model by disrupting the AMPK-mTOR signal cascade [48]. More recently, α7nAchR activation was shown to prevent ischemia/reperfusion-induced blood-brain barrier damage via regulating autophagy [49]. These studies are consistent with our findings that GTS-21 and PNU increase AMPK-mTOR signaling in the brain and gut tissues. Based on these reports, our data suggested that α7nAchR activation by GTS-21 and PNU may improve autophagy-dependent α-syn clearance, thereby improving nigrostriatal dopaminergic degeneration.

Previous research has shown that α7nAChR regulates the innate immune system and has a role in the cholinergic anti-inflammatory pathway [50,51]. α7nAChR has been found to exert an

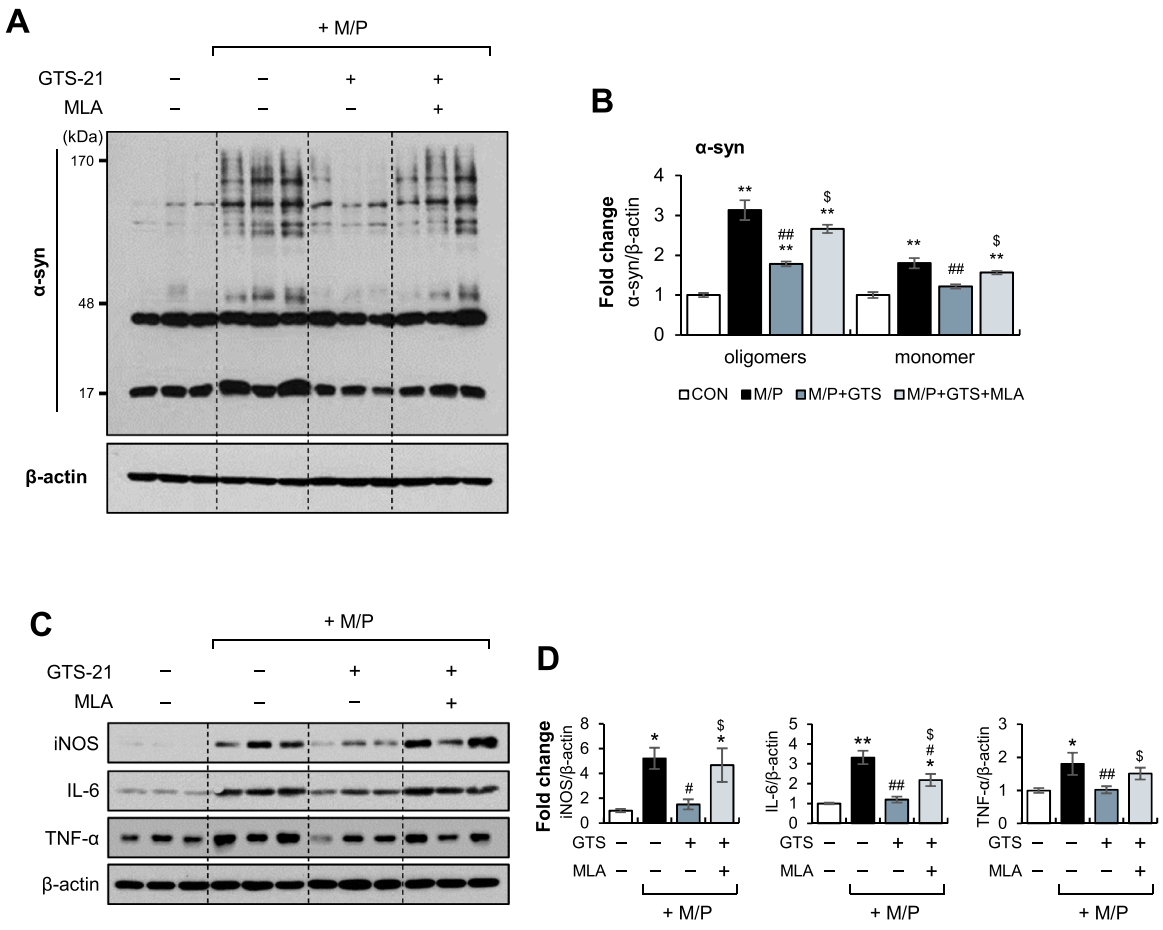


Fig. 9. MLA pretreatment abolished the GTS-21-elicited reduction in α-syn oligomer species and expression of proinflammatory markers in the distal colon area of subacute MPTP mice. A. MLA pretreatment reversed the GTS-induced reduction in the levels of α-syn oligomer species in the colon area (each group N = 4–6). **B.** Diagram showing the quantification of the levels of α-syn oligomer and monomer species. **C.** MLA pretreatment reversed the GTS-induced decrease in the levels of iNOS, IL-6, and TNF-α in the colon area of MPTP mice (each group N = 4–6). **D.** Diagram showing the quantification of the levels of iNOS, IL-6, and TNF-α. Data are expressed as the mean ± SEM. * $^{*}p < 0.01$ vs. CON; $^{\#}p < 0.05$ and $^{\#\#}p < 0.01$ vs. M/P; $^{\$}p < 0.05$ vs. M/P + GTS.

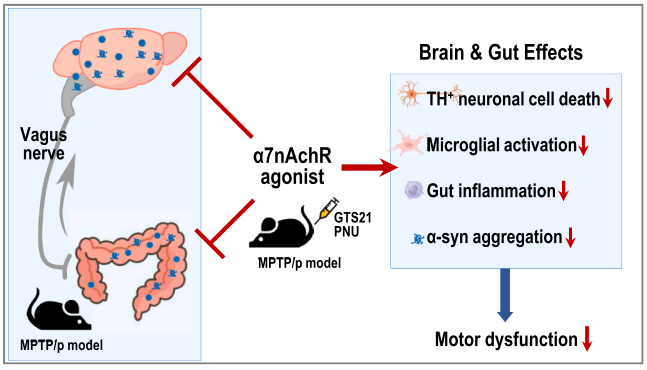


Fig. 10. Scheme for the effects of α7nAchR activation in the brain and gut of the MPTP/P mouse model. In our experimental paradigm, α7nAchR agonists GTS-21 and PNU protected dopaminergic neurons in the substantia nigra par compacta from neurotoxin effects. α7nAchR activation reduces α-syn aggregation and inflammation in the brain and gut. The brain-gut effects may improve the motor dysfunction of PD mice.

anti-inflammatory activity in numerous cell types, including human monocytes, macrophages, microglia, astrocytes, disease animal models or patients with sepsis, pancreatitis, rheumatoid arthritis, and neurological disorders such as Alzheimer's disease, cerebral ischemia, and PD [52–58]. For example, GTS-21 suppressed the expression of proinflammatory mediators such as TNF-α via inhibiting NF-κB activity and activating the Nrf2 pathway in LPS-stimulated microglia and astrocytes [29,59]. A recent study by our group reported that GTS-21 exerted anti-inflammatory effects in LPS-induced neuroinflammation and acute MPTP model mice [60]. The Nrf2/ARE and PKA/CREB pathways were shown to be mainly involved in the anti-inflammatory/neuroprotective effects of GTS-21. Considering that inflammation plays a crucial role in α-syn aggregation and transmission [61], activating the cholinergic anti-inflammatory signaling pathway may be a promising strategy for treating PD and other α-synucleionpathies.

5. Conclusions

This study is the first to investigate the role of α7nAchR activation in PD-related pathophysiology in the brain and gut. The α7nAChR agonists, GTS-21 and PNU, improved α-syn clearance and reduced inflammation in both the brain and gut of a subacute MPTP mouse model of PD. Hence, GTS-21- and PNU-stimulated α7nAChR activation could potentially prevent and treat PD.

Funding

This research was supported by a National Research Foundation of Korea (NRF) grant funded by the Korean government (MSIT) (Grant No. NRF-2020R1A5A2019210).

CRediT authorship contribution statement

Leem Yea-Hyun: Writing – original draft, Investigation, Data curation, Conceptualization. **Park Jung-Eun:** Investigation, Data curation, Conceptualization. **Park Jin-Sun:** Methodology, Investigation, Data curation. **Kim Do-Yeon:** Investigation, Data curation. **Park Jae-Min:** Investigation, Data curation. **Kim Seong-Eun:** Investigation, Data curation. **Kang Jihee Lee:** Supervision. **Kim Hee-Sun:** Writing – review & editing, Conceptualization.

Declaration of Competing Interest

The authors declare that they have no conflicts of interest.

Appendix A. Supporting information

Supplementary data associated with this article can be found in the online version at doi:10.1016/j.biopha.2025.117871.

Data availability

Data will be made available on request.

References

[1] W. Poewe, K. Seppi, C.M. Tanner, G.M. Halliday, P. Brundin, J. Volkmann, A. Schrag, A.E. Lang, Parkinson disease, Nat. Rev. Dis. Prim. 3 (2017) 17013.
[2] J.T. Bendor, T.P. Logan, R.H. Edwards, The function of α-synuclein, Neuron 79 (6) (2013) 1044–1066.
[3] J. Burr, The synaptic function of α-synuclein, J. Park. 'S. Dis. 5 (4) (2015) 699–713.
[4] S. Petrucci, M. Ginevrino, E.M. Valente, Phenotypic spectrum of alpha-synuclein mutations: New insights from patients and cellular models, Park. Relat. Disord. 22 (2016) S16–S20.
[5] C. Schiesling, N. Kieper, K. Seidel, R. Kruger, Familial Parkinson's disease: genetics, clinical phenotype and neuropathology in relation to the common sporadic form of the disease, Neuropathol. Appl. Neurobiol. 34 (2008) 255–271.
[6] A. Bose, M.F. Beal, Mitochondrial dysfunction in Parkinson's disease, J. Neurochem. 139 (2013) 216–231.
[7] T. Sohrabi, B. Mirzaei-Behbahani, R. Zadail, M. Pirhaghi, L.A. Morozova-Roche, A. A. Meratan, Common mechanisms underlying α-synuclein-induced mitochondrial dysfunction in Parkinson's disease, J. Mol. Biol. 435 (2023) 167992.
[8] Y.C. Wong, D. Krainc, α-synuclein toxicity in neurodegeneration: mechanism and therapeutic strategies, Nat. Med. 23 (3) (2017) 1–13.
[9] P. Borghammer, How does Parkinson's disease begin? Perspectives on neuroanatomical pathways, prions, and histology, Mov. Disord. 33 (1) (2018) 48–57.
[10] P. Brundin, R. Melki, Prying into the prion hypothesis for Parkinson's disease, J. Neurosci. 37 (41) (2017) 9808–9818.
[11] P. Desplats, H. Lee, E. Bae, C. Patrick, E. Rockenstein, L. Crews, B. Spencer, E. Masliah, S. Lee, Inclusion formation and neuronal cell death through neuron-to-neuron transmission of alpha-synuclein, Proc. Natl. Acad. Sci. U. S. A. 106 (31) (2009) 13010–13015.
[12] C. Hansen, E. Angot, A. Bergström, J.A. Steiner, L. Pieri, G. Paul, T.F. Outeiro, R. Melki, P. Kallunki, K. Fog, J. Li, P. Brundin, α-Synuclein propagates from mouse brain to grafted dopaminergic neurons and seeds aggregation in cultured human cells, J. Clin. Invest. 121 (2) (2011) 715–725.
[13] H.J. Lee, J.E. Suk, E.J. Bae, S.J. Lee, Clearance and deposition of extracellular alpha-synuclein aggregates in microglia, Biochem. Biophys. Res. Commun. 372 (2008) 423–428.
[14] M. Goedert, M.G. Spillantini, K. Del Tredici, H. Braak, 100 years of Lewy pathology, Nat. Rev. Neurol. 9 (1) (2013) 13–24.
[15] H. Braak, K.Del Tredici, U. Rüb, R.A. de Vos, E.N. Jansen Steur, E. Braak, Staging of brain pathology related to sporadic Parkinson's disease, Neurobiol. Aging 24 (2) (2003) 197–211.
[16] M.G. Cersosimo, E.E. Benarroch, Pathological correlates of gastrointestinal dysfunction in Parkinson's disease, Neurobiol. Dis. 46 (3) (2012) 559–564.
[17] H. Braak, E. Ghebremedhin, U. Rüb, H. Bratzke, K. Del Tredici, Stages in the development of Parkinson's disease-related pathology, Cell Tissue Res 318 (1) (2004) 121–134.
[18] C.D. Rietdijk, P. Perez-Pardo, J. Garssen, R.J. van Wezel, A.D. Kraneveld, Exploring Braak's hypothesis of Parkinson's disease, Front. Neurol. 8 (2017) 37.
[19] M.L. Muller, N.I. Bohnen, Cholinergic dysfunction in Parkinson's disease, Curr. Neurol. Neurosci. Rep. 13 (2013) 377.
[20] S. Perez-Lloret, M.C. Peralta, F.J. Barrantes, Pharmacotherapies for Parkinson's disease symptoms related to cholinergic degeneration, Expert Opin. Pharmacother. 17 (2016) 2405–2415.
[21] R.A. Travagli, K.N. Browning, M. Camilleri, Parkinson's disease and the gut: new insights into pathogenesis and clinical relevance, Nat. Rev. Gastroenterol. Hepatol. 17 (2020) 676–685.
[22] J. Zhao, Y. Li, Y. Li, S. Xu, T. Tao, Y. Hua, J. Zhang, Y. Fan, Activation of α7-nAChRs promotes the clearance of α-synuclein and protects against apoptotic cell death induced by exogenous α-synuclein fibrils, Front. Cell Dev. Biol. 9 (2021) 637319.
[23] K.J. Tracey, The inflammatory reflex, Nature 420 (2002) 853–859.
[24] L.V. Borovikova, S. Ivanova, M. Zhang, H. Yang, G.I. Botchkina, L.R. Watkins, H. Wang, N. Abumrad, J.W. Eaton, K.J. Tracey, Vagus nerve stimulation attenuates the systemic inflammatory response to endotoxin, Nature 405 (6785) (2000) 458–462.
[25] K.J. Tracey, Fat meets the cholinergic anti-inflammatory pathway, J. Exp. Med. 202 (2005), 1071-1021.
[26] K.J. Tracey, Physiology and immunology of the cholinergic anti-inflammatory pathway, J. Clin. Invest. 117 (2007) 289.
[27] W.R. Kem, V.M. Mahnir, L. Prokai, R.L. Papke, X. Cao, S. LeFrancois, K. Wildeboer, K. Prokai-Tatrai, J. Porter-Papke, F. Soti, Hydroxy metabolites of the Alzheimer's drug candidate 3-[(2,4-dimethoxy)benzylidene]-anabaseine dihydrochloride (GTS-21): their molecular properties, interactions with brain nicotinic receptors, and brain penetration, Mol. Pharmacol. 65 (1) (2004) 56–67.
[28] K. Takata, T. Amamiya, H. Mizoguchi, S. Kawanishi, E. Kuroda, R. Kitamura, A. Ito, Y. Saito, M. Tawa, T. Nagasawa, H. Okamoto, Y. Sugino, S. Takegami, T. Kitade, Y. Toda, W.R. Kem, Y. Kitamura, S. Shimohama, E. Ashihara, Alpha7 nicotinic acetylcholine receptor-specific agonist DMXBA (GTS-21) attenuates Abeta accumulation through suppression of neuronal gamma-secretase activity and promotion of microglial amyloid-beta phagocytosis and ameliorates cognitive impairment in a mouse model of Alzheimer's disease, Neurobiol. Aging 62 (2018) 197–209.
[29] M.S. Thomsen, J.D. Mikkelsen, The α7 nicotinic acetylcholine receptor ligands methyllycaconitine, NS6740 and GTS-21 reduce lipopolysaccharide-induced TNF-α release from microglia, J. Neuroimmunol. 251 (1-2) (2012) 65–72.
[30] J.P. Redrobe, E.Ø. Nielsen, J.K. Christensen, D. Peters, D.B. Timmermann, G. M. Olsen, Alpha7 nicotinic acetylcholine receptor activation ameliorates scopolamine-induced behavioural changes in a modified continuous Y-maze task in mice, Eur. J. Pharmacol. 602 (1) (2009) 58–65.
[31] V. Stuckenholz, M. Bacher, M. Balzer-Geldsetzer, D. Alvarez-Fischer, W.H. Oertel, R.C. Dodel, C. Noelker, The alpha7 nAChR agonist PNU-282987 reduces inflammation and MPTP-induced nigral dopaminergic cell loss in mice, J. Park. Dis. 3 (2) (2013) 161–172.
[32] Y. Jiang, H. Ma, X. Wang, Z. Wang, Y. Yang, L. Li, T. Feng, Protective Effect of the alpha7 Nicotinic Receptor Agonist PNU-282987 on Dopaminergic Neurons Against 6-Hydroxydopamine, Regulating Anti-neuroinflammatory and the Immune Balance Pathways in Rat, Front, Aging Neurosci. 12 (2021) 606927.
[33] S. Schneider, A. Gruart, S. Grade, Y. Zhang, S. Kröger, F. Kirchhoff, G. Eichele, J. M. Delgado, L. Dimou, Decrease in newly generated oligodendrocytes leads to motor dysfunctions and changed myelin structures that can be rescued by transplanted cells, Glia 64 (2018) 2201–2218.
[34] Y.H. Leem, J.S. Park, J.E. Park, D.Y. Kim, H.S. Kim, Neurogenic effects of rotarod walking exercise in subventricular zone, subgranular zone, and substantia nigra in MPTP-induced Parkinson's disease mice, Sci. Rep. 12 (1) (2022) 10544.
[35] M. Jucker, L.C. Walker, Self-propagation of pathogenic protein aggregates in neurodegenerative diseases, Nature 501 (7465) (2013) 45–51.
[36] C. Challis, A. Hori, T.R. Sampson, B.B. Yoo, R.C. Challis, A.M. Hamilton, S. K. Mazmanian, L.A. Volpicelli-Daley, V. Gradinaru, Gut-seeded α-synuclein fibrils promote gut dysfunction and brain pathology specifically in aged mice, Nat. Neurosci. 23 (3) (2020) 327–336.
[37] S. Holmqvist, O. Chutna, L. Bousset, P. Aldrin-Kirk, W. Li, T. Björklund, Z. Wang, L. Roybon, R. Melki, J. Li, Direct evidence of Parkinson pathology spread from the gastrointestinal tract to the brain in rats, Acta Neuropathol. 128 (6) (2014) 805–820.
[38] S. Kim, S.H. Kwon, T.I. Kam, N. Panicker, S.S. Karuppagounder, S. Lee, J.H. Lee, W. R. Kim, M. Kook, C.A. Foss, C. Shen, H. Lee, S. Kulkarni, P.J. Pasricha, G. Lee, M. G. Pomper, V.L. Dawson, T.M. Dawson, H.S. Ko, Transneuronal propagation of pathologic α-synuclein from the gut to the brain models Parkinson's disease, Neuron 103 (4) (2019) 627–641.e7.
[39] N. Uemura, H. Yagi, M.T. Uemura, Y. Hatanaka, H. Yamakado, R. Takahashi, Inoculation of α-synuclein preformed fibrils into the mouse gastrointestinal tract induces Lewy body-like aggregates in the brainstem via the vagus nerve, Mol. Neurodegener. 13 (1) (2018) 21.
[40] K. Ono, M. Hirohata, M. Yamada, Anti-fibrillogenic and fibril-destabilizing activity of nicotine in vitro: implications for the prevention and therapeutics of Lewy body diseases, Exp. Neurol. 205 (2) (2007) 414–424.
[41] J. Kardani, R. Sethi, I. Roy, Nicotine slows down oligomerisation of α-synuclein and ameliorates cytotoxicity in a yeast model of Parkinson's disease, Biochim. Biophys. Acta Mol. Basis Dis 1863 (6) (2017) 1454–1463.
[42] F. Bono, V. Mutti, P. Savoia, A. Barbon, A. Bellucci, C. Missale, C. Fiorentini, Nicotine prevents alpha-synuclein accumulation in mouse and human iPSC-derived dopaminergic neurons through activation of the dopamine D3-acetylcholine nicotinic receptor heteromer, Neurobiol. Dis. 129 (2019) 1–12.
[43] A. Djajadikerta, S. Keshri, M. Pavel, R. Prestil, L. Ryan, D.C. Rubinsztein, Autophagy induction as a therapeutic strategy for neurodegenerative diseases, J. Mol. Biol. 432 (2020) 2799–2821.
[44] E. Wong, A.M. Cuervo, Autophagy gone awry in neurodegenerative diseases, Nat. Neurosci. 13 (2010) 805–811.

[45] F. Limanaqi, F. Biagioni, S. Gambardella, P. Familiari, A. Frati, F. Fornai, Promiscuous roles of autophagy and proteasome in neurodegenerative proteinopathies, Int. J. Mol. Sci. 21 (2020) 28.
[46] D. Ebrahimi-Fakhari, I. Cantuti-Castelvetri, Z. Fan, E. Rockenstein, E. Masliah, B. T. Hyman, P.J. McLean, V.K. Unni, Distinct roles in vivo for the ubiquitin-proteasome system and the autophagy-lysosomal pathway in the degradation of α-synuclein, J. Neurosci. 31 (2011) 14508–14520.
[47] M.R. Pollmanns, J. Beer, I. Rosignol, N. Rodriguez-Muela, B.H. Falkenburger, E. Dinter, Activated endolysosomal cation channel TRPML1 facilitates maturation of α-synuclein-containing autophagosomes, Front. Cell. Neurosci. 16 (2022) 861202.
[48] B.Z. Shao, S.L. Wang, J. Fang, Z.S. Li, Y. Bai, K. Wu, Alpha7 nicotinic acetylcholine receptor alleviates inflammatory bowel disease through induction of AMPK-mTOR-p70S6K-mediated autophagy, Inflammation 42 (2019) 1666–1679.
[49] F. Gao, W. Du, C. Gua, P. Geng, W. Liu, X. Jin, α7 nAch receptor, a promising target to reduce BBB damage by regulating inflammation and autophagy after ischemic stroke, Biomed. Pharmacother. 179 (2024) 117337.
[50] R. Gamage, I. Wagnon, I. Rossetti, R. Childs, G. Niedermayer, R. Chesworth, E. Gyengesi, Cholinergic modulation of glial function during aging and chronic neuroinflammation, Front. Cell. Neurosci. 14 (2020) 577912.
[51] M. Reale, E. Costantini, Cholinergic modulation of the immune system in neuroinflammatory diseases, Diseases 9 (2021) 29.
[52] J. Egea, I. Buendia, E. Parada, E. Navarro, R. Leon, M.G. Lopez, Anti-inflammatory role of microglial alpha7 nAChRs and its role in neuroprotection, Biochem. Pharmacol. 97 (2015) 463–472.
[53] F.A. Koopman, P.R. Schuurman, M.J. Vervoordeldonk, P.P. Tak, Vagus nerve stimulation: a new bioelectronics approach to treat rheumatoid arthritis? Best. Pract. Res. Clin. Rheumatol. 28 (2014) 625–635.
[54] W.R. Parrish, M. Rosas-Ballina, M. Gallowitsch-Puerta, M. Ochani, K. Ochani, L. H. Yang, L.Q. Hudson, X. Lin, N. Patel, S.M. Johnson, S. Chavan, R.S. Goldstein, C. J. Czura, E.J. Miller, Y. Al-Abed, K.J. Tracey, V.A. Pavlov, Modulation of TNF release by choline requires alpha7 subunit nicotinic acetylcholine receptor-mediated signaling, Mol. Med. 14 (2008) 567–574.
[55] M. Rosas-Ballina, R.S. Goldstein, M. Gallowitsch-Puerta, L. Yang, S.I. Valdés-Ferrer, N.B. Patel, S. Chavan, Y. Al-Abed, H. Yang, K.J. Tracey, The selective alpha7 agonist GTS-21 attenuates cytokine production in human whole blood and human monocytes activated by ligands for TLR2, TLR3, TLR4, TLR9, and RAGE, Mol. Med. 15 (2009) 195–202.
[56] Y. Zhou, X. Zuo, Y. Li, Y. Wang, H. Zhao, S. Xiao, Nicotine inhibits tumor necrosis factor-α induced IL-6 and IL-8 secretion in fibroblast-like synoviocytes from patients with rheumatoid arthritis, Rheumatol. Int. 32 (2012) 97–104.
[57] X. Liu, Z. Mei, J. Qian, Y. Zeng, M. Wang, Puerarin partly counteracts the inflammatory response after cerebral ischemia/reperfusion via activating the cholinergic anti-inflammatory pathway, Neural Regen. Res. 8 (2013) 3203–3215.
[58] D.J. Van Westerloo, I.A. Giebelen, S. Florquin, M.J. Bruno, G.J. Larosa, L. Ulloa, K. J. Tracey, T. van der Poll, The vagus nerve and nicotinic receptors modulate experimental pancreatitis severity in mice, Gastroenterology 130 (2006) 1822–1830.
[59] H. Patel, J. McIntire, S. Ryan, A. Dunah, R. Loring, Anti-inflammatory effects of astroglial α7 nicotinic acetylcholine receptors are mediated by inhibition of the NF-kB pathway and activation of the Nrf2 pathway, J. Neuroinflamm. 14 (2017) 192.
[60] J.E. Park, Y.H. Leem, J.S. Park, D.Y. Kim, J.L. Kang, H.S. Kim, Anti-Inflammatory and Neuroprotective Mechanisms of GTS-21, an α7 Nicotinic Acetylcholine Receptor Agonist, in Neuroinflammation and Parkinson's Disease Mouse Models, Int. J. Mol. Sci. 23 (8) (2022) 4420.
[61] T. Zheng, Z. Zhang, Activated microglia facilitate the transmission of α-synuclein in Parkinson's disease, Neurochem. Int. 148 (2021) 105094.